LA-UR-01-2458

c.1

TITLE: BENCH TEST OF A RESIDUAL GAS IONIZATION PROFILE MONITOR (RGIPM)

AUTHOR(S):

William C. Sellyey	LANSCE-1
J. Douglas Gilpatrick	LANSCE-1
Ralph Senior	General Atomics, San Diego CA

SUBMITTED TO: DIPAC
May 13 - May 15
Grenoble, France

Los Alamos
NATIONAL LABORATORY

Form No. 836 R5
ST 2629 10/91

Bench Test of a Residual Gas Ionization Profile Monitor (RGIPM)[1].

W. C. Sellyey, J. D. Gilpatrick, LANL, Los Alamos NM, USA
Ralph Senior, General Atomics, San Diego CA, USA

Abstract

An RGIPM has been designed[1], constructed and bench tested to verify that all components are functioning properly and that the desired resolution of about 50 μm rms can be achieved. This paper will describe some system details and it will compare observed results to detailed numerical calculations of expected detector response.

1 BEAMLINE COMPONENTS

Figure 1 shows a top view horizontal cross section of the primary beam line components. It is set up to measure a vertical beam profile. The magnet (1) is a split H configuration with a gap of 24.6 cm. The coils (2) can produce a 0.12 T field at the center of the magnet. The electrostatic vacuum box (3) contains an 8 mm thick high voltage (HV) plate (4) 39 by 38 cm. One cm above the plate (towards the bottom of the page) is a set of 100 μm gold coated wires (not seen) running across the page. These are separated by 30 mm. High voltage feedthrough (5) is used to supply up to -15 kV to the plate and (6) supplies voltage to the grid wires. The vacuum box is at ground potential. Not seen is a 100 μW Krypton light and collimator on the top of the box. It shines a 5° wide beam on the wires near the center of the box. Its spectrum consists of 20% 10.64 eV photons and 80% 10.03 eV photons. On the left and right side of the box are flanges (not shown) to connect to 10 cm diameter beam tubes.

A removable "hat" (7) contains a mechanism that moves a scintillation detector (8) across the wires (in and

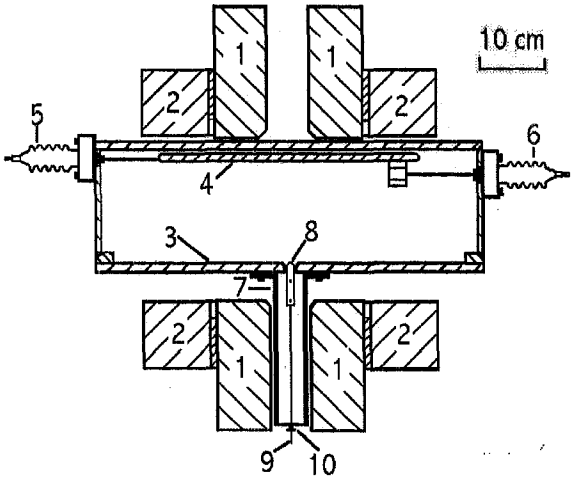

Figure 1. Major Beam Line Components

out of the page). A quartz fibre (9) carries scintillation photons through an optical vacuum feedthrough (10). A motion feedthrough under the hat (not visible) connects the moving mechanism to a worm gear driven by a stepper motor. The worm gear shaft was rigidly connected to an LVDT.

Some details of the scintillation detector are shown in figure 2. The limiting aperture (1) was a 125 μm hole in a 1 mm thick Aluminium piece. The electrons that pass through this hit a 0.5 mm thick, 2X2 mm square scintillator (2). A 500 μm gold coated quartz optical fibre (3) caries some of the resulting photons to a photomultiplier (PM) tube outside the vacuum. The detector moves in a 1.8 cm by 10 cm slot in the top of the vacuum box. The total distance from the HV plate to the scintillator is 14 cm.

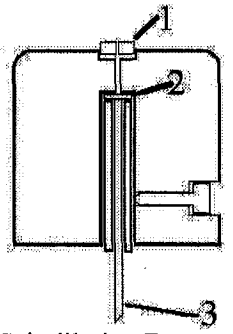

Figure 2. Scintillation Detector

2 DATA ACQUISITION SYSTEM

The single photon PM output pulses are amplified, shaped and sent as TTL pulses to a counter/timer on a National Instruments (NI) PCI-MIO-16XE-10 board. This board is installed in a Micron PC. A/D's and D/A's on the NI board are used for controlling and measuring most voltages and currents in the system.

High voltages are generated by analogue control of Glassman MJ series power supplies. A high precision resistive high voltage divider system is used to produce a stable ratio of voltages to the plate and grid. The exact ratio of the grid to plate voltage is fine tuned by a manually controlled potentiometer.

The stepper motor is controlled by a set of output bits on the NI board. The LVDT electronics is interfaced to the PC by a serial port. Software closes the loop between the stepper motor and the LVDT. The detector position is reproducible to about 3 μm on a short term basis (hours and a few degrees C temperature change). All control and display software is written in LabVIEW.

3 DATA

Photoelectrons are guided to the detector by the parallel electric and magnetic fields. The detector is scanned across this distribution and this results in a count rate distribution that is a convolution of the detector aperture and the electron distribution. Figure 3 shows a typical scan with a magnetic field of 0.12 T, a plate high voltage of 9 kV and grid potentiometer setting of 50 kΩ. The figure shows two sets of data. One is the actual scan and the second is background correction data. The background correction data was taken by moving the detector back to the starting position of the scan after every third data point. Data set acquisition time was typically several hours.

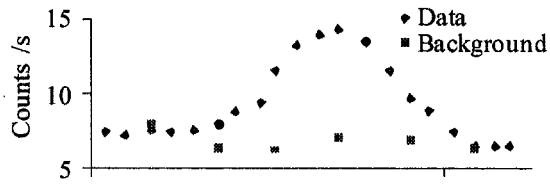

Figure 3. A Profile. B field =0.1 T, E field =64.5k V/m, grid potentiometer=50 k.

Figure 4 shows all the (scaled) background corrected measured areas for scans taken at a 0.12 T magnetic field, 9 kV plate voltage while varying the grid potentiometer. The potentiometer rate of change is 12.85 divisions per volt. The actual grid voltage is to be defined below and is initially treated as unknown.

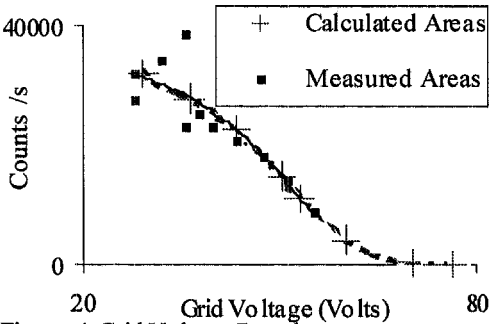

Figure 4. Grid Voltage Results.

4 THEORY

Software was written to describe the process that the photoelectrons go through from the time they absorb the energy of a photon, to when they arrive at the GSO scintillator. The first part of the program traces the electrons in the gold of the 100 μm wire and is Monte Carlo based[2]. The photons arrive at the wire with random positions across (up and down the page in figure 1) the wire. The photon penetration depth was calculated as -30.3ln(x) Å where x is a random number between 0 and 1. A single electron in the Fermi sea absorbs the full energy restriction that it started out in the Fermi sea. The bottom of the Fermi well is taken at 8.22 eV, and the depth of the Fermi distribution is 3.4 eV. The density of states of the electrons is assumed to vary as $E^{1/2}$. The electron moves through the metal, loosing energy through collisions with other electrons and phonons. The energy loss process due to phonon collisions is taken to be the same as that experienced by electrons at the top of the Fermi distribution during the electrical conduction process[3]. This is characterised by a relaxation length l=410 Å and the electron velocity decays as exp(-x/l) where x is the distance the electron travelled.

The average separation of the conduction electrons is 2.57 Å. Thus the moving electron is always interacting with many electrons. To simulate this, the electron is taken as undergoing a collision every -2.57ln(x) Å, where x is a random number. The collision is treated as Rutherford scattering in the center of mass of the two electrons with two quantum mechanical restrictions. The first is that both of the electrons after the collision have to be above the Fermi level. The second sets a limit on the minimum size of the impact parameter[4] $b=\hbar/p$ where p is the initial momentum in the relative frame. The electron with the larger energy after the collision is taken as the scattered incoming electron. The electron is stepped through the gold until either its kinetic energy drops below the well potential depth value of 8.22 eV, or it reaches the surface with enough of a kinetic energy component perpendicular to the surface to escape.

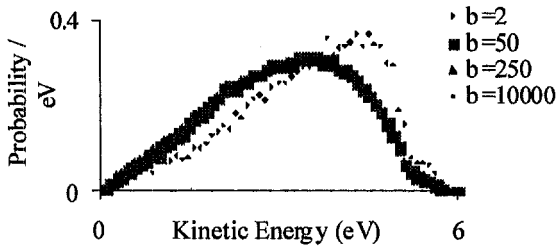

Figure 5. Energy Distribution as a Function of Impact Parameter b.

Figure 5 shows the energy distribution of electrons for different upper limits on the impact parameter in units of average electron separation. It can be seen that at 50 and above, the value of the maximum impact parameter does not matter. Most calculations were done using a maximum impact parameter of 250.

Once an electron leaves the metal, its motion is determined by the uniform magnetic field, and an initially rapidly changing electric field. The path of the electrons is traced to the detector using F=ma in 0.1 ps steps.

The electric field can be well approximated by considering it as being made up of two independent components. The first component is calculated by considering the wire as being in a uniform electric field perpendicular to its axis. The uniform field is calculated

distance. The second component is obtained by considering the cylindrical wire with an applied voltage 1 cm above the grounded (infinite) plate. If the wires were not present, the electrons would see a linear voltage change as they moved through the plate to the detector gap. If now the wires are introduced at 1 cm from the plate, and their potential is adjusted so that it is the same as the potential that existed at their location before they were introduced, the electric field near the wires will be described by only the first term. The second term is determined by the deviation from this potential and results in a field outside the wire described by two line charges: one located at the center of the wire and an equal and opposite sign charge one cm inside the plate. This potential deviation will be referred to as the grid voltage. In principle, this can be calculated from the resistor values in the voltage divider and detailed knowledge of the geometry. However it more accurately measured as described below.

For every plate voltage there is a minimum positive grid voltage that stops all the electrons leaving the wire. This can be calculate numerically by requiring the highest kinetic energy electrons velocity drop to zero at the same location the electric field becomes zero along a line perpendicular to the plate and passing through the wire center. For a 9 kV plate voltage this is 77.9 V and the stopping point is 200 μm from the wire centrer.

Another way to do this is to use the program described above to calculate the number of electrons that reach the detector for 10^7 photoelectrons. This is shown in figure 3 along with a 6th order fit. A 2nd order fit to the scaled measured count rates for various grid voltages is also shown. When these were first plotted on the graph, they did not coincide with the calculated numbers. To obtain the relation between grid voltage and potentiometer setting the experimental count rate line is scaled vertically (this is the same as changing the UV light intensity) and displaced horizontally until it overlaps the calculated curve. This process produces a grid voltage for every measurement on the graph.

5 DATA ANALYSIS

The position distribution obtained with the software described above was convolved with the expected shape of the collimator in front of the GSO scintillator. The obvious initial choice for this shape is a d=125 μm radius circle. However this does not produce acceptable results.

The construction of the moving mechanism is such that it could readily be tilted in the direction of motion. This is simulated by two overlapping circles with their centers displaced with respect to each other. The aperture is the overlapping part of the circles. Shown in figure 6 is the data of figure 3 and fitted to it is a (normalised) convolution of this type for a grid voltage of 36 V with shown is an additional set of data taken at the same grid voltage with a fitted convolution using a displacement of 0.4d (χ^2=.0.7). The area under this second set of data with circle separation of .4d should be much larger than for .9d. At this time this is an unexplained discrepancy.

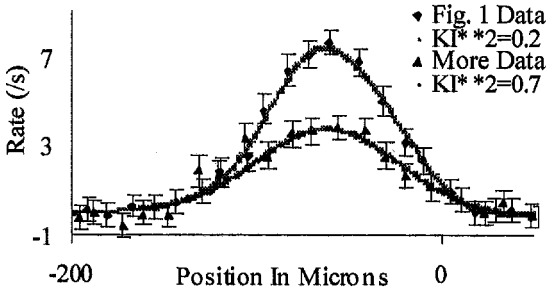

Figure 6. Fit To Two Profiles.

The statistical errors in the count rates are typically about 0.1 count per second. A straight line fit to the background data of figure 3 results in average deviations from the line of 0.5/s. This was added in quadrature for all data and is presumably due to things like photomultiplier dark current, electronic drift, and cosmic radiation. The detector assembly is guided by two linear bearings on two parallel shafts. The assembly is attached to the linear drive mechanism at a point midway between these bearings and 2.5 cm from the scintillator. The bearings are lose enough so the assembly can wobble in the direction of motion. This results in two correlated errors. The first is caused by a change in the separation in the overlapping circles. The other happens only on the leading and trailing edge of a profile. As the detector assembly pivots around the point where it is attached to the drive, the scintillator moves at the end of a 2.5 cm arm. This will case a count rate variation that adds to the first on one side of a profile, and subtracts on the other side. It was assumed that addition occurs on the leading edge because most of the data shows more scatter here. An rms wobble of .01° was assumed for the analysis in figure 6.

All profile measurements done with B=0.12 T, E=64.5 kV/m resulted in rms resolutions of between 27 and 44 μm.

REFERENCES

[1] W. C. Sellyey, J. D. Gilpatrick, "A Compact Residual Gas Ionization Profile Monitor System", Proceedings of the 1999 PAC, 2152.

[2] M. Kotera, Y. Kamiya, "Computer Simulation of Light by High Energy Electrons in YAG Single Crystals", Ultramicroscopy, 54 (1994) 293.

[3] M. A. Omar, "Elementary Solid State Physics: Principles And Applications", Addison-Wesley, 1975, 157.

[4] J. D. Jackson, "Classical Electrodynamics", John Wiley & Sons, 1963, 440.